Supplementary Information

An Unexpected All-Metal Aromatic Tetranuclear Silver Cluster in Human Copper Chaperone Atox1

Xiuxiu Wang[a, b], Zong-Chang Han[c], Wei Wei*[a, b, f], Hanshi Hu[c], Pengfei Li [d], Peiqing Sun[b], Xiangzhi Liu[a], Zhijia Lv[g], Feng Wang[g], Yi Cao[d], Zijian Guo*[a, b, e], Jun Li*[c,h] and Jing Zhao*[a, b, e, f]

[a.] *State Key Laboratory of Coordination Chemistry, Chemistry and Biomedicine Innovation Center (ChemBIC), School of Chemistry and Chemical Engineering, Nanjing University, Nanjing 210023, China.*

[b.] *School of Life Sciences, Nanjing University, Nanjing 210023, China.*

[c.] *Department of Chemistry and Key Laboratory of Organic Optoelectronics & Molecular Engineering of Ministry of Education, Tsinghua University, Beijing 100084, China.*

[d.] *National Laboratory of Solid State Microstructure, Department of Physics, Nanjing University, Nanjing 210023, China.*

[e.] *Nanchuang (Jiangsu) Institute of Chemistry and Health, Nanjing 210023, China.*

[f.] *Shenzhen Research Institute, Nanjing University, Shenzhen, 518000, China.*

[g.] *Elias James Corey Institute of Biomedical Research, Wuxi Biortus Biosciences Co., Ltd, Jiangyin, 214437, China.*

[h.] *Department of Chemistry, Southern University of Science and Technology, Shenzhen 518055, China*

Experimental

Protein Sample preparation for Single-molecule AFM. Glasses were first immersed into chromic acid for 2h to remove impurities. After rinsing with Mili-Q water, glasses was covered by silane-PEG-NHS solution in DMSO (Nanocs inc, 5kDa,1mg ml^{-1}) for 2h. Glasses were rinsed with large amount of DMSO to remove the unreacted silane-PEG-NHS. Then glassed was covered by NH_2-BG solution in DMSO (10μg ml^{-1}) for 2h, so protein snap can directly bind to glasses. Finally, rinsing glasses with Mili-Q water to remove unreacted NH_2-BG. Glasses was used immediately after finishing the modification process. For cantilever was coated by Au, protein cys-Xmod-doc can directly bind on it.

Crystallization. Crystal screening was performed at 293 K by the sitting-drop vapour-diffusion method. A 200 nanolitre protein solution (27 mg/mL) was mixed with 200 nanolitre reservoir solution and equilibrated against 30 microlitre reservoir solution. Commercial crystallization kits from Hampton Research and Qiagen were used for crystal screening. Initial crystals of Atox1 were observed under the following condition: 0.2 M tri-sodium citrate, 20 % (w/v) PEG 3350. Single crystals were obtained by further optimization of salt concentration and pH values. For heavy atom derivative crystals preparation, we added 5 mM AgNO3 to a cryo-protection solution (0.2 M tri-sodium citrate, 20 % (w/v) PEG 3350, 25% glycerol), soaked the crystals for about 4 hours and then the data were collected at home source diffraction system. For Crystal optimizing, protein was incubated with 5mM TCEP and 5mM AgNO3 on ice for 3 hours. A 200 nanolitre protein solution (29 mg/mL) was mixed with 180 nanolitre reservoir solution and 20 nanolitre lysozyme seed, and equilibrated against 15 microlitre reservoir solution. Final crystals of Atox1 were observed under the following condition: 0.2M LiCl, 0.1M Tris pH 8, 20% PEG 6,000. For heavy atom derivative crystals preparation, we added 5 mM AgNO3 and 5 mM TCEP to a reservoir solution (0.2M LiCl, 0.1M Tris pH 8, 20% PEG 6,000), soaked the crystals for about 4 hours, and then added 5 mM AgNO3 to a cryo-protection solution. The data were collected at SSRF BL18U1.

The contents of the unit cell were analysed using the Matthews coefficient (Matthews, 1968). Molecular replacements were performed using MOLREP (Vagin & Teplyakov, 2010) and Phaser (McCoy, 2007). The models were refined by iterative cycles of manual building using Coot (Emsley *et al*., 2010) followed by simulated annealing. Subsequent stages of refinement were carried out with REFMAC5 (Murshudov *et al*., 2011) within the CCP4 suite (Winn *et al*., 2011; Collaborative Computational Project, Number 4, 1994) and manual improvement in Coot. All structural representations were generated using PyMOL (DeLano, 2002) with subsequent ray tracing.

Protein expression. The DNA fragment encoding the Homo sapiens protein Atox1 protein was synthesis by Nanjing GenScript Biotechnology Corporation. The fusion protein 6×His-TEV-Atox1 was sub-cloned into a pET28a vector by standard polymerase chain reaction (PCR) methods, and the resulting construct was subsequently transformed into BL21 (DE3) cells. The fusion protein was expressed in LB medium containing 50 μg/mL kanamycin after induction with 1 mM IPTG at 15℃. To obtain purified Atox1, *E.coli* BL21 (DE3) cells containing the recombinant plasmid that had been cultured overnight were collected by centrifugation. The pellet was re-suspended in buffer (50 mM Tris-HCl pH 7.0, 500 mM NaCl and 5% v/v glycerol) and dissociated by microfluid. The supernatant was obtained by centrifuging the cell lysate at 20,000 rpm and 277 K for 1 h. Standard Ni-affinity chromatography (His-Trap FF) was performed for preliminary purification of the His-tagged fusion protein from the supernatant. The enrichment fusion protein was digested by TEV

protease at 277 K overnight. Ni-affinity chromatography (His Trap HP) was used again to obtain Atox1, which was separated from the 6×His -TEV fusion protein. High purity Atox1 was obtained after further purified by size-exclusion chromatography (Superdex 30) and was concentrated.

For the loop bypass mutant, the sequence of Coh-(GB1)4-Atox1-linker-Atox1-(GB1)4-Snap is as follows:

Coh:

MGTALTDRGMTYDLDPKDGSSAATKPVLEVTKKVFDTAADAAGQTVTVEFKVSGAEGKYATTGYHIYWDER
LEVVATKTGAYAKKGAALEDSSLAKAENNGNGVFVASGADDDFGADGVMWTVELKVPADAKAGDVYPIDV
AYQWDPSKGDLFTDNKDSAQGKLMQAYFFTQGIKSSSNPSTDEYLVKANATYADGYIAIKAGEP

GB1:

MDTYKLILNGKTLKGETTTEAVDAATAEKVFKQYANDNGVDGEWTYDDATKTFTVTE

ATOX1:

MPKHEFSVDMTCGGCAEAVSRVLNKLGGVKYDIDLPNKKVCIESEHSMDTLLATLKKTGKTVSYLGLE

Linker:

RSGGSGGSGGSGGSGGSGGSGGSGGSGGSGGSGGSGGSGGSGGSGGSGGSGGSRS

Snap：

GGGMDKDCEMKRTTLDSPLGKLELSGCEQGLHEIKLLGKGTSAADAVEVPAPAAVLGGPEPLMQATAWLNA
YFHQPEAIEEFPVPALHHPVFQQESFTRQVLWKLLKVVKFGEVISYQQLAALAGNPAATAAVKTALSGNPVPILI
PCHRVVSSSGAVGGYEGGLAVKEWLLAHEGHRLGKPGLGPA

Cys-Xmod-Doc:

CGGNTVTSAVKTQYVEIESVDGFYFNTEDKFDTAQIKKAVLHTVYNEGYTGDDGVAVVLREYESEPVDITAEL
TFGDATPANTYKAVENKFDYEIPVYYNNATLKDAEGNDATVTVYIGLKGDTDLNNIVDGRDATATLTYYAAT
STDGKDATTVALSPSTLVGGNPESVYDDFSAFLSDVKVDAGKELTRFAKKAERLIDGRDASSILTFYTKSSVDQ
YKDMAANEPNKLWDIVTGDA

Mass Spectrometry. Proteins were injected into a reverse phase HPLC (Agilent 1200 series HPLC, Agilent Technologies) with a ProSwift™ RP-3U LC Column (4.6×50 mm, SS, Thermo Scientific™). Positive ion Electrospray Ionization (ESI) mass spectra for intact protein were obtained with an Agilent 6224 mass spectrometer equipped with an ESI interface and a time-of-flight (TOF) mass detector (Agilent Technologies). Mass spectra were analyzed and deconvoluted using an Agilent software MassHunter version B.04.00 (Agilent Technologies).

Inductively coupled plasma mass spectrometry (ICP-MS) experiments. To confirm the binding condition of Atox1 fusion protein and Ag, we conducted ICP-MS detection in a 220 μl complex solution containing Atox1 fusion protein and Ag. As a result, we found that the molar ratio of Ag (0.278×10^{-6} mol) and Atox1 (0.064×10^{-6} mol) was about 4.34 in Ag-Atox1 complex.

Single-molecule AFM experiments. Single-molecule AFM experiments were carried out on a commercial AFM (Force Robot 300, JPK, Berlin, Germany). All the force-extension experiments were carried out in Tris-HCl buffer (25mM Tris, 72mM NaCl). Protein sample (0.1mg ml^{-1},150μl) was directly deposited on a freshly cleaved glass surface for 2h and was washed with buffer to remove unreacted protein. We modified the cantilever tip with cys-Xmod-doc. The gold-coated

cantilever was immersed in a protein solution (0.1 mg ml^{-1}) for 1 hour at room temperature to allow the formation of gold-thiol linkage. The physically adsorbed proteins were removed by rinsing the cantilever tip with deionized water for at least 5 times in an incubator. Then, the sample chamber was filled with 1ml buffer before the measurement. The spring constant of the AFM cantilevers (Biolever-RC-150VB-70 from Olympus) was calibrated using the equipartition theorem before each experiment, with a typical value of 6pN nm^{-1}. The pulling speed was 400 nm s^{-1} for all traces.

EPR measurement. 0.2 mM Atox1 was incubated with 10 molar equivalents of AgNO3 in 20 mM Tris buffer containing 200 mM NaCl. Then the spin-trapping agent 5,5-dimethylpyrroline-N-oxide (DMPO) was added to the reaction mixture. After shaking for 1 minute, the sample was transferred to a quartz capillary tube. For MTSSL labeling, 0.2 mM Atox1 was incubated with 10 molar equivalents of MTSSL overnight at 4°C. Then the reaction mixture was added to Ni-NTA to remove free spin label. The continuous-wave electron paramagnetic resonance (CW-EPR) spectra were recorded on a Bruker A300 spectrometer (Bruker Biospin GmbH, Rheinstetten, Germany) at X-band (9.5 GHz).

Crystallization. Crystal screening was performed at 293 K by the sitting-drop vapour-diffusion method. A 200 nanolitre protein solution (27 mg/mL) was mixed with 200 nanolitre reservoir solution and equilibrated against 30 microlitre reservoir solution. Commercial crystallization kits from Hampton Research and Qiagen were used for crystal screening. Initial crystals of Atox1 were observed under the following condition: 0.2 M tri-sodium citrate, 20 % (w/v) PEG 3350. Single crystals were obtained by further optimization of salt concentration and pH values. For heavy atom derivative crystals preparation, we added 5 mM AgNO3 to a cryo-protection solution (0.2 M tri-sodium citrate, 20 % (w/v) PEG 3350, 25% glycerol), soaked the crystals for about 4 hours and then the data were collected at home source diffraction system.

Crystal optimizing was performed at 293 K by the sitting-drop vapour-diffusion method. Protein was incubated with 5mM TCEP and 5mM AgNO3 on ice for 3 hours. A 200 nanolitre protein solution (29 mg/mL) was mixed with 180 nanolitre reservoir solution and 20 nanolitre lysozyme seed, and equilibrated against 15 microlitre reservoir solution. Final crystals of Atox1 were observed under the following condition: 0.2M LiCl, 0.1M Tris pH 8, 20% PEG 6,000. For heavy atom derivative crystals preparation, we added 5 mM AgNO3 and 5 mM TCEP to a reservoir solution (0.2M LiCl, 0.1M Tris pH 8, 20% PEG 6,000), soaked the crystals for about 4 hours, and then added 5 mM AgNO3 to a cryo-protection solution. The data were collected at SSRF BL18U1.

The contents of the unit cell were analysed using the Matthews coefficient (Matthews, 1968). Molecular replacements were performed using MOLREP (Vagin & Teplyakov, 2010) and Phaser (McCoy, 2007). The models were refined by iterative cycles of manual building using Coot (Emsley *et al*., 2010) followed by simulated annealing. Subsequent stages of refinement were carried out with REFMAC5 (Murshudov *et al*., 2011) within the CCP4 suite (Winn *et al*., 2011; Collaborative Computational Project, Number 4, 1994) and manual improvement in Coot. All structural representations were generated using PyMOL (DeLano, 2002) with subsequent ray tracing.

Theoretical Analyses and Computational Modeling.

In Figure 3, the electronic structure of Ag_4^{2+} cluster based on the experimentally measured geometry (Figure 2) have been investigated using density functional theory (DFT) with Amsterdam Density Functional 2019 program. The calculations were done using PBE exchange-correlation functional and the TZP Slater basis sets. Frozen core

approximation was applied to the [$1s^2$…$4p^6$] core of Ag, and Zeroth-Order Regular Approximation to the Dirac Equation (ZORA) was used to account for the scalar relativistic (SR) effect.

The constrained DFT geometry optimization was done at the level of SR-ZORA PBE/DZP with Grimme D3-BJ Dispersion Correction. The model of constrained geometry optimization adopted $[Ag_4]^{q+}$ cluster inside the frozen experimental cavity, with size about 5 Å around the $[Ag_4]^{q+}$ core. The calculated molecular orbital (MO) energy levels and wavefunctions of Ag_4^{2+} cluster are listed in Table S3-S5, which were analyzed using Hückel method based on three kinds of geometry structures with T_d, D_{4h} and D_{2h} symmetry. The MO energies and frontier MOs of optimized geometry structures with T_d, D_{4h} and D_{2h} symmetries and experimentally measured structure with C_2 symmetry were studied by ADF 2019 program with level of PBE/TZP, frozen core approximation and ZORA scalar relativistic method.

The ELF color-filled map and multicenter bond index were calculated using Gaussian-16B and Multiwfn-3.8 at the level of PBE0/def2-TZVP. The nucleus-independent chemical shift (NICS) of Ag_4^{2+} cluster based on the experimentally measured geometry was studied using Multiwfn and Gaussian with level of B3LYP/def2-SVP.

Cartesian Coordinates of Geometry Structures

Experimental structure of Ag_4-(Atox1)$_2$ 7DC1:

Ag	-27.203000	46.371000	7.945000
Ag	-29.133000	45.802000	9.934000
Ag	-26.557000	46.744000	11.514000
Ag	-25.099000	48.131000	9.525000
N	-28.361000	48.860000	4.792000
C	-27.081000	49.589000	4.574000
C	-25.891000	48.627000	4.676000
C	-26.964000	50.740000	5.578000
O	-27.127000	50.312000	6.930000
H	-26.820000	51.001000	7.524000
H	-28.777896	49.166964	5.647553
H	-25.999884	51.192138	5.473347
N	-26.071000	47.402000	5.159000
C	-24.953000	46.440000	5.296000
C	-25.498000	45.017000	5.233000

O	-26.714000	44.871000	5.238000
C	-24.180000	46.719000	6.596000
S	-24.925000	46.060000	8.125000
H	-24.091000	47.800000	6.706000
H	-26.998000	47.118000	5.441000
H	-24.248000	46.558000	4.473000
H	-23.226000	46.203000	6.487000
N	-24.615000	44.048000	5.170000
H	-23.638879	44.256229	5.231875
N	-25.498000	42.692000	7.408000
C	-26.141000	42.143000	8.613000
C	-27.660000	42.282000	8.539000
O	-28.391000	41.595000	9.364000
H	-25.782175	42.669416	9.472669
H	-24.658993	43.170734	7.666614
N	-28.155000	43.145000	7.656000
C	-29.605000	43.435000	7.533000
C	-30.366000	42.201000	7.022000
O	-31.598116	42.083025	7.249031
C	-29.860000	44.677000	6.684000
S	-29.519000	46.245000	7.532000
H	-30.906000	44.674000	6.379000
H	-27.514000	43.625000	7.041000
H	-29.993000	43.662000	8.526000
H	-29.173000	44.624000	5.839000
N	-31.221000	40.627000	10.217000

C	-32.130000	41.528000	10.972000
C	-31.685000	42.966000	10.843000
H	-31.594000	43.409000	11.835000
H	-30.419820	41.001675	9.750384
H	-32.124594	41.248882	12.004939
H	-32.419000	43.523000	10.261000
H	-30.719000	43.003000	10.339000
C	-33.325000	48.376000	9.028000
C	-31.958000	47.762000	8.859000
N	-30.957000	48.407000	9.735000
H	-30.670000	47.758000	10.454000
H	-34.059238	47.741331	8.577457
H	-31.645000	47.875000	7.821000
H	-33.540104	48.486214	10.070345
H	-32.022000	46.709000	9.134000
H	-30.154000	48.677000	9.186000
H	-27.840000	49.445000	9.220000
H	-28.104000	48.893000	10.664000
O	-31.111000	46.252000	11.542000
H	-30.238000	45.932000	11.782000
H	-31.435000	45.761000	10.784000
N	-28.134000	48.991000	14.667000
C	-29.405000	48.247000	14.885000
C	-29.167000	46.736000	14.783000
C	-30.460000	48.722000	13.881000
O	-30.008000	48.649000	12.529000

H	-30.047000	49.522000	12.131000
H	-27.715817	48.692270	13.809163
H	-31.334040	48.113718	13.985628
N	-28.016000	46.279000	14.300000
C	-27.742000	44.830000	14.163000
C	-26.237000	44.590000	14.226000
O	-25.502000	45.571000	14.221000
C	-28.370000	44.300000	12.863000
S	-27.427000	44.616000	11.334000
H	-29.351000	44.763000	12.753000
H	-27.307000	46.940000	14.018000
H	-28.197000	44.279000	14.986000
H	-28.399000	43.216000	12.971000
N	-25.839000	43.341000	14.289000
H	-26.507184	42.599581	14.227122
N	-24.223000	43.428000	12.051000
C	-23.426000	43.710000	10.846000
C	-22.787000	45.095000	10.920000
O	-21.827000	45.385000	10.095000
H	-24.061230	43.662325	9.986285
H	-25.219626	43.373298	11.989804
N	-23.287000	45.955000	11.803000
C	-22.813000	47.356000	11.926000
C	-21.364000	47.398000	12.437000
O	-20.645759	48.406067	12.210060
C	-23.761000	48.198000	12.775000

S	-25.290000	48.687000	11.927000
H	-23.235000	49.103000	13.080000
H	-24.023000	45.640000	12.418000
H	-22.816000	47.806000	10.933000
H	-24.058000	47.576000	13.620000
N	-19.574000	47.352000	9.242000
C	-19.899000	48.589000	8.487000
C	-21.367000	48.923000	8.616000
H	-21.697000	49.462000	7.728000
H	-20.357313	46.730866	9.217233
H	-19.660005	48.444394	7.454106
H	-21.523000	49.544000	9.498000
H	-21.941000	48.002000	8.715000
C	-25.232000	53.048000	10.431000
C	-25.384000	51.557000	10.600000
N	-26.443000	51.013000	9.724000
H	-26.739000	50.112000	10.072000
H	-24.315127	53.366371	10.881427
H	-25.638000	51.342000	11.638000
H	-26.085000	50.911000	8.785000
H	-25.219998	53.289418	9.388660
H	-24.440000	51.086000	10.325000
O	-28.102000	48.675000	9.730000
O	-24.500000	50.069000	7.917000
H	-24.854000	49.476000	8.584000
H	-24.476000	50.964000	8.264000

O	-28.468000	51.143000	11.618000
H	-28.631000	51.743000	10.887000
H	-28.219000	50.281000	11.276000
H	-19.317839	49.400287	8.872961
H	-18.781616	46.905970	8.825845
H	-31.410458	39.645987	10.175530
H	-33.123137	41.430587	10.585878
H	-24.918352	43.101477	5.060124
H	-25.276182	41.946486	6.779506
H	-25.887694	41.107471	8.704739
H	-33.345573	49.336101	8.556107
H	-28.983998	49.045776	4.032157
H	-27.093978	50.003599	3.587674
H	-27.713832	51.469906	5.354642
H	-20.965998	46.570093	12.985693
H	-23.767818	43.291125	12.930815
H	-22.655830	42.972869	10.754481
H	-24.867553	43.130722	14.398882
H	-29.848057	41.442364	6.473268
H	-25.482274	48.523065	3.692618
H	-25.150599	49.102190	5.285017
H	-29.281473	46.330082	15.766375
H	-29.948755	46.332473	14.173964
H	-29.757537	48.465496	15.871345
H	-27.507097	48.809032	15.424549
H	-30.716503	49.736480	14.104463

H -26.053039 53.545990 10.903018

Optimized structure of $[Ag_4]^{4+}$ in constrained 7DC1 cavity :

Ag -27.174248 46.886293 7.647061

Ag -28.912106 45.580500 9.744174

Ag -26.811643 46.856738 11.823799

Ag -24.848644 47.709082 9.780124

N -28.361000 48.860000 4.792000

C -27.081000 49.589000 4.574000

C -25.891000 48.627000 4.676000

C -26.964000 50.740000 5.578000

O -27.127000 50.312000 6.930000

H -26.820000 51.001000 7.524000

H -28.777896 49.166964 5.647553

H -25.999884 51.192138 5.473347

N -26.071000 47.402000 5.159000

C -24.953000 46.440000 5.296000

C -25.498000 45.017000 5.233000

O -26.714000 44.871000 5.238000

C -24.180000 46.719000 6.596000

S -24.925000 46.060000 8.125000

H -24.091000 47.800000 6.706000

H -26.998000 47.118000 5.441000

H -24.248000 46.558000 4.473000

H -23.226000 46.203000 6.487000

N -24.615000 44.048000 5.170000

H -23.638879 44.256229 5.231875

N	-25.498000	42.692000	7.408000
C	-26.141000	42.143000	8.613000
C	-27.660000	42.282000	8.539000
O	-28.391000	41.595000	9.364000
H	-25.782175	42.669416	9.472669
H	-24.658993	43.170734	7.666614
N	-28.155000	43.145000	7.656000
C	-29.605000	43.435000	7.533000
C	-30.366000	42.201000	7.022000
O	-31.598116	42.083025	7.249031
C	-29.860000	44.677000	6.684000
S	-29.519000	46.245000	7.532000
H	-30.906000	44.674000	6.379000
H	-27.514000	43.625000	7.041000
H	-29.993000	43.662000	8.526000
H	-29.173000	44.624000	5.839000
N	-31.221000	40.627000	10.217000
C	-32.130000	41.528000	10.972000
C	-31.685000	42.966000	10.843000
H	-31.594000	43.409000	11.835000
H	-30.419820	41.001675	9.750384
H	-32.124594	41.248882	12.004939
H	-32.419000	43.523000	10.261000
H	-30.719000	43.003000	10.339000
C	-33.325000	48.376000	9.028000
C	-31.958000	47.762000	8.859000

N	-30.957000	48.407000	9.735000
H	-30.670000	47.758000	10.454000
H	-34.059238	47.741331	8.577457
H	-31.645000	47.875000	7.821000
H	-33.540104	48.486214	10.070345
H	-32.022000	46.709000	9.134000
H	-30.154000	48.677000	9.186000
H	-27.840000	49.445000	9.220000
H	-28.104000	48.893000	10.664000
O	-31.111000	46.252000	11.542000
H	-30.238000	45.932000	11.782000
H	-31.435000	45.761000	10.784000
N	-28.134000	48.991000	14.667000
C	-29.405000	48.247000	14.885000
C	-29.167000	46.736000	14.783000
C	-30.460000	48.722000	13.881000
O	-30.008000	48.649000	12.529000
H	-30.047000	49.522000	12.131000
H	-27.715817	48.692270	13.809163
H	-31.334040	48.113718	13.985628
N	-28.016000	46.279000	14.300000
C	-27.742000	44.830000	14.163000
C	-26.237000	44.590000	14.226000
O	-25.502000	45.571000	14.221000
C	-28.370000	44.300000	12.863000
S	-27.427000	44.616000	11.334000

H	-29.351000	44.763000	12.753000
H	-27.307000	46.940000	14.018000
H	-28.197000	44.279000	14.986000
H	-28.399000	43.216000	12.971000
N	-25.839000	43.341000	14.289000
H	-26.507184	42.599581	14.227122
N	-24.223000	43.428000	12.051000
C	-23.426000	43.710000	10.846000
C	-22.787000	45.095000	10.920000
O	-21.827000	45.385000	10.095000
H	-24.061230	43.662325	9.986285
H	-25.219626	43.373298	11.989804
N	-23.287000	45.955000	11.803000
C	-22.813000	47.356000	11.926000
C	-21.364000	47.398000	12.437000
O	-20.645759	48.406067	12.210060
C	-23.761000	48.198000	12.775000
S	-25.290000	48.687000	11.927000
H	-23.235000	49.103000	13.080000
H	-24.023000	45.640000	12.418000
H	-22.816000	47.806000	10.933000
H	-24.058000	47.576000	13.620000
N	-19.574000	47.352000	9.242000
C	-19.899000	48.589000	8.487000
C	-21.367000	48.923000	8.616000
H	-21.697000	49.462000	7.728000

H	-20.357313	46.730866	9.217233
H	-19.660005	48.444394	7.454106
H	-21.523000	49.544000	9.498000
H	-21.941000	48.002000	8.715000
C	-25.232000	53.048000	10.431000
C	-25.384000	51.557000	10.600000
N	-26.443000	51.013000	9.724000
H	-26.739000	50.112000	10.072000
H	-24.315127	53.366371	10.881427
H	-25.638000	51.342000	11.638000
H	-26.085000	50.911000	8.785000
H	-25.219998	53.289418	9.388660
H	-24.440000	51.086000	10.325000
O	-28.102000	48.675000	9.730000
O	-24.500000	50.069000	7.917000
H	-24.854000	49.476000	8.584000
H	-24.476000	50.964000	8.264000
O	-28.468000	51.143000	11.618000
H	-28.631000	51.743000	10.887000
H	-28.219000	50.281000	11.276000
H	-19.317839	49.400287	8.872961
H	-18.781616	46.905970	8.825845
H	-31.410458	39.645987	10.175530
H	-33.123137	41.430587	10.585878
H	-24.918352	43.101477	5.060124
H	-25.276182	41.946486	6.779506

H	-25.887694	41.107471	8.704739
H	-33.345573	49.336101	8.556107
H	-28.983998	49.045776	4.032157
H	-27.093978	50.003599	3.587674
H	-27.713832	51.469906	5.354642
H	-20.965998	46.570093	12.985693
H	-23.767818	43.291125	12.930815
H	-22.655830	42.972869	10.754481
H	-24.867553	43.130722	14.398882
H	-29.848057	41.442364	6.473268
H	-25.482274	48.523065	3.692618
H	-25.150599	49.102190	5.285017
H	-29.281473	46.330082	15.766375
H	-29.948755	46.332473	14.173964
H	-29.757537	48.465496	15.871345
H	-27.507097	48.809032	15.424549
H	-30.716503	49.736480	14.104463
H	-26.053039	53.545990	10.903018

Optimized structure of $[Ag_4]^{2+}$ in constrained 7DC1 cavity :

Ag	-27.189764	47.238952	7.715822
Ag	-28.860772	45.762323	9.769021
Ag	-27.301700	47.134770	11.812722
Ag	-25.130535	47.709555	9.787557
N	-28.361000	48.860000	4.792000
C	-27.081000	49.589000	4.574000

C	-25.891000	48.627000	4.676000
C	-26.964000	50.740000	5.578000
O	-27.127000	50.312000	6.930000
H	-26.820000	51.001000	7.524000
H	-28.777896	49.166964	5.647553
H	-25.999884	51.192138	5.473348
N	-26.071000	47.402000	5.159000
C	-24.953000	46.440000	5.296000
C	-25.498000	45.017000	5.233000
O	-26.714000	44.871000	5.238000
C	-24.180000	46.719000	6.596000
S	-24.925000	46.060000	8.125000
H	-24.091000	47.800000	6.706000
H	-26.998000	47.118000	5.441000
H	-24.248000	46.558000	4.473000
H	-23.226000	46.203000	6.487000
N	-24.615000	44.048000	5.170000
H	-23.638879	44.256229	5.231876
N	-25.498000	42.692000	7.408000
C	-26.141000	42.143000	8.613000
C	-27.660000	42.282000	8.539000
O	-28.391000	41.595000	9.364000
H	-25.782175	42.669416	9.472670
H	-24.658993	43.170734	7.666614
N	-28.155000	43.145000	7.656000
C	-29.605000	43.435000	7.533000

C	-30.366000	42.201000	7.022000
O	-31.598116	42.083025	7.249031
C	-29.860000	44.677000	6.684000
S	-29.519000	46.245000	7.532000
H	-30.906000	44.674000	6.379000
H	-27.514000	43.625000	7.041000
H	-29.993000	43.662000	8.526000
H	-29.173000	44.624000	5.839000
N	-31.221000	40.627000	10.217000
C	-32.130000	41.528000	10.972000
C	-31.685000	42.966000	10.843000
H	-31.594000	43.409000	11.835000
H	-30.419820	41.001675	9.750384
H	-32.124594	41.248882	12.004940
H	-32.419000	43.523000	10.261000
H	-30.719000	43.003000	10.339000
C	-33.325000	48.376000	9.028000
C	-31.958000	47.762000	8.859000
N	-30.957000	48.407000	9.735000
H	-30.670000	47.758000	10.454000
H	-34.059238	47.741331	8.577458
H	-31.645000	47.875000	7.821000
H	-33.540104	48.486214	10.070346
H	-32.022000	46.709000	9.134000
H	-30.154000	48.677000	9.186000
H	-27.840000	49.445000	9.220000

H	-28.104000	48.893000	10.664000
O	-31.111000	46.252000	11.542000
H	-30.238000	45.932000	11.782000
H	-31.435000	45.761000	10.784000
N	-28.134000	48.991000	14.667000
C	-29.405000	48.247000	14.885000
C	-29.167000	46.736000	14.783000
C	-30.460000	48.722000	13.881000
O	-30.008000	48.649000	12.529000
H	-30.047000	49.522000	12.131000
H	-27.715817	48.692270	13.809163
H	-31.334040	48.113718	13.985628
N	-28.016000	46.279000	14.300000
C	-27.742000	44.830000	14.163000
C	-26.237000	44.590000	14.226000
O	-25.502000	45.571000	14.221000
C	-28.370000	44.300000	12.863000
S	-27.427000	44.616000	11.334000
H	-29.351000	44.763000	12.753000
H	-27.307000	46.940000	14.018000
H	-28.197000	44.279000	14.986000
H	-28.399000	43.216000	12.971000
N	-25.839000	43.341000	14.289000
H	-26.507184	42.599581	14.227122
N	-24.223000	43.428000	12.051000
C	-23.426000	43.710000	10.846000

C	-22.787000	45.095000	10.920000
O	-21.827000	45.385000	10.095000
H	-24.061230	43.662325	9.986285
H	-25.219626	43.373298	11.989804
N	-23.287000	45.955000	11.803000
C	-22.813000	47.356000	11.926000
C	-21.364000	47.398000	12.437000
O	-20.645759	48.406067	12.210060
C	-23.761000	48.198000	12.775000
S	-25.290000	48.687000	11.927000
H	-23.235000	49.103000	13.080000
H	-24.023000	45.640000	12.418000
H	-22.816000	47.806000	10.933000
H	-24.058000	47.576000	13.620000
N	-19.574000	47.352000	9.242000
C	-19.899000	48.589000	8.487000
C	-21.367000	48.923000	8.616000
H	-21.697000	49.462000	7.728000
H	-20.357313	46.730866	9.217233
H	-19.660005	48.444394	7.454106
H	-21.523000	49.544000	9.498000
H	-21.941000	48.002000	8.715000
C	-25.232000	53.048000	10.431000
C	-25.384000	51.557000	10.600000
N	-26.443000	51.013000	9.724000
H	-26.739000	50.112000	10.072000

H	-24.315127	53.366371	10.881427
H	-25.638000	51.342000	11.638000
H	-26.085000	50.911000	8.785000
H	-25.219998	53.289418	9.388660
H	-24.440000	51.086000	10.325000
O	-28.102000	48.675000	9.730000
O	-24.500000	50.069000	7.917000
H	-24.854000	49.476000	8.584000
H	-24.476000	50.964000	8.264000
O	-28.468000	51.143000	11.618000
H	-28.631000	51.743000	10.887000
H	-28.219000	50.281000	11.276000
H	-19.317839	49.400287	8.872961
H	-18.781616	46.905970	8.825845
H	-31.410458	39.645987	10.175530
H	-33.123137	41.430587	10.585878
H	-24.918352	43.101477	5.060124
H	-25.276182	41.946486	6.779506
H	-25.887694	41.107471	8.704739
H	-33.345573	49.336101	8.556107
H	-28.983998	49.045776	4.032157
H	-27.093978	50.003599	3.587674
H	-27.713832	51.469906	5.354642
H	-20.965998	46.570093	12.985693
H	-23.767818	43.291125	12.930815
H	-22.655830	42.972869	10.754481

H	-24.867553	43.130722	14.398882
H	-29.848057	41.442364	6.473268
H	-25.482274	48.523065	3.692618
H	-25.150599	49.102190	5.285017
H	-29.281473	46.330082	15.766375
H	-29.948755	46.332473	14.173964
H	-29.757537	48.465496	15.871345
H	-27.507097	48.809032	15.424549
H	-30.716503	49.736480	14.104463
H	-26.053039	53.545990	10.903018

Experimental structure (C_2) of Ag_4 Cluster:

Ag	-0.514904	-1.748836	0.236102
Ag	-2.305118	0.390645	-0.236102
Ag	0.514904	1.748836	0.236102
Ag	2.305118	-0.390645	-0.236102

Optimized T_d-$[Ag_4]^{2+}$ Cluster:

Ag	1.060049	-1.060049	1.060049
Ag	-1.060049	1.060049	1.060049
Ag	-1.060049	-1.060049	-1.060049
Ag	1.060049	1.060049	-1.060049

Optimized D_{4h}-$[Ag_4]^{2+}$ Cluster:

Ag	-1.469085	-1.469085	0.000000
Ag	-1.469085	1.469085	0.000000
Ag	1.469085	-1.469085	0.000000
Ag	1.469085	1.469085	0.000000

Optimized D_{2h}-$[Ag_4]^{2+}$ Cluster:

Ag	2.692548	0.000000	0.000000
Ag	0.000000	1.448782	0.000000
Ag	0.000000	-1.448782	0.000000
Ag	-2.692548	0.000000	0.000000

Optimized D_{4h}-$[C_4H_4]^{2+}$ Cluster:

C	0.000000	0.952783	0.000000
C	0.000000	0.0000000	1.061328
C	0.000000	-0.952783	0.000000
C	0.000000	0.000000	-1.061328
H	0.000000	2.040396	0.000000
H	0.000000	-2.040396	0.000000
H	0.000000	0.000000	2.129351
H	0.000000	0.000000	-2.129351

Table S1. Strengths of single metal− ligand bonds in protein or nonprotein surfaces

Single thiol-matal bond	protein	ref
Au-S	**~165 pN**	[1]
Cu-S	**~171 pN**	[1]
Zn-S	**~170pN**	[2]
Zn-S	**~90pN**	[3]
Fe-S	**~211pN**	[4]
Fe-N	**~160 pN**	[5]
Fe-O	**~127 pN**	[6]
Ag-S	**~64 pN Atox1**	**This work**

Table S2. Crystallization Method

Protein	Atox1 for 5F0W	Atox1 for 7DC1
Method	Sitting-drop vapour-diffusion	Sitting-drop vapour-diffusion
Plate type	Corning 3552	Corning 3552
Temperature (K)	293	293
Protein concentration	27 mg/mL	29 mg/mL
Buffer composition of protein solution	50 mM Tris-HCl pH 7.5, 150 mM NaCl, 1 mM TCEP	50 mM Tris-HCl pH 7.5, 150 mM NaCl, 1 mM TCEP
Composition of reservoir solution	0.2 M tri-sodium citrate, 20 % (w/v) PEG 3350	0.2M LiCl, 0.1M Tris pH 8, 20% (w/v) PEG 6,000
Volume and ratio of drop	200 nL protein/200 nL reservoir	200 nL protein/200 nL reservoir
Volume of reservoir	microlitre.	microlitre.

Table S3. X-ray data collection and refinement statistics

We finished all of the data collection works by use F-RE++ and R-AXIS IV of RIGAKU.

Data collection	**5F0W**	**7DC1**
Space group	$P6_2$	$P3_221$
Cell dimensions		
a,b,c(Å)	112.49, 112.49, 56.63	104.49 104.493 29.188
α,β,γ(°)	90.00, 90.00, 120.00	90.000 90.000 120.000
Resolution	50.00-2.70 (2.75-2.70)*	19.47-1.75 (1.78-1.75)
R_{merge}	12.9(43.7)	5.6 (61.6)
$I/\sigma I$	17.78(4.68)	17.0 (2.3)
Completeness(%)	90.2(87.4)	98.5 (97.1)
Redundancy	6.2(6.3)	4.6 (4.3)
Refinement		
Resolution(Å)	24.48-2.70	19.47-1.75
No. unique reflections	10336	18311 (1002)
R_{work} / R_{free}	0.26/0.29	0.18/0.20
No. atoms		
Protein	2056	1019
Ligand/ion	8	4
Water	12	133
B-factors		
Protein	31.55	28.44
Ligand/ion	38.73	27.41
Water	23.05	39.01
R.m.s.deviations		
Bond lengths	0.014	0.005
Bond angles	1.62	1.259

*Values in parentheses are for highest-resolution shell.

Table S4. The Hückel MO energies and MO wavefunctions of planar D_{2h}-Ag_4 cluster.

MO	Eigenvalue	Energy	Eigenfunctions
LUMO+2(a_g)	$\chi 4 = 1.5616$	α-1.5616β	$\Psi_4=(0.4352\phi_1+0.4352\phi_2-0.5573\phi_3-0.5573\phi_4)$
LUMO+1(a_u)	$\chi 3 = 1.0000$	$\alpha-\beta$	$\Psi_3=(0.7071\phi_1-0.7071\phi_2)$
LUMO(b_u)	$\chi 2 = 0.0000$	α	$\Psi_2=(-0.7071\phi_3+0.7071\phi_4)$
HOMO(a_g)	$\chi 1 = -2.5616$	α+2.5616β	$\Psi_1=(0.5573\phi_1+0.5573\phi_2+0.4352\phi_3+0.4352\phi_4)$

Table S5. The Hückel MO energies and wavefunctions of square planar D_{4h}-Ag_4 cluster.

MO	Eigenvalue	Energy	Eigenfunctions
LUMO+1(a_g)	$\chi 4 = 2.0000$	α-2.0000β	$\Psi_4=(0.5000\phi_1-0.5000\phi_2+0.5000\phi_3-0.5000\phi_4)$
LUMO(b_{2u})	$\chi 3 = 0.0000$	α	$\Psi_3=(0.7071\phi_1-0.7071\phi_3)$
LUMO(b_{1u})	$\chi 2 = 0.0000$	α	$\Psi_2=(0.7071\phi_2-0.7071\phi_4)$
HOMO(a_g)	$\chi 1 = -2.0000$	α+2.0000β	$\Psi_1=(0.5000\phi_1+0.5000\phi_2+0.5000\phi_3+0.5000\phi_4)$

Table S6. The Hückel MO energies and wavefunctions of the tetrahedron T_d-Ag_4 cluster.

MO	Eigenvalue	Energy	Eigenfunctions
LUMO(t_2)	$\chi 4 = 1.0000$	α-1.0000β	$\Psi_4=(0.5000\phi_1-0.5000\phi_2+0.5000\phi_3-0.5000\phi_4)$
LUMO(t_2)	$\chi 3 = 1.0000$	α-1.0000β	$\Psi_3=(0.5000\phi_1+0.5000\phi_2-0.5000\phi_3-0.5000\phi_4)$
LUMO(t_2)	$\chi 2 = 1.0000$	α-1.0000β	$\Psi_2=(0.5000\phi_1-0.5000\phi_2-0.5000\phi_3+0.5000\phi_4)$
HOMO(a_1)	$\chi 1 = -3.0000$	α+3.0000β	$\Psi_1=(0.5000\phi_1+0.5000\phi_2+0.5000\phi_3+0.5000\phi_4)$

Table S7. The MO contours and energy of the frontier MOs of T_d, D_{4h}, D_{2h} and the C_2 experimental measured structures $[Ag_4]^{2+}$ cluster (isosurface = 0.03 a.u.) .

MO diagram E / Hartree	**T_d** 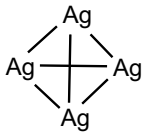	**D_{4h}** 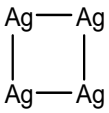	**C_2, Exp** 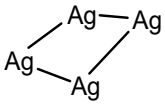	**D_{2h}** 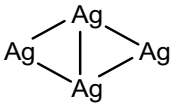
LUMO+2	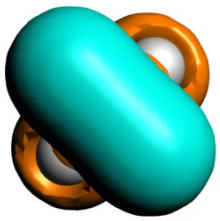 t_2, E = -0.4406	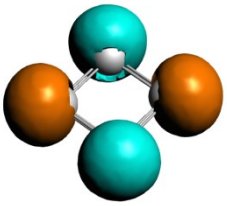 b_{2g}, E = -0.3784	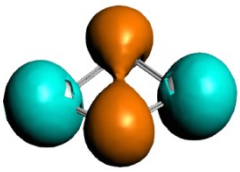 a, E = -0.3859	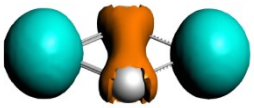 a_g, E = -0.3961
LUMO+1	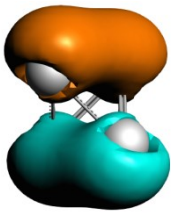 t_2, E = -0.4406	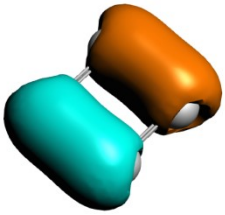 e_{1u}, E = -0.4611	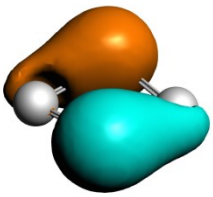 b, E = -0.4450	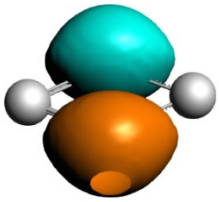 b_u, E = -0.4247
LUMO	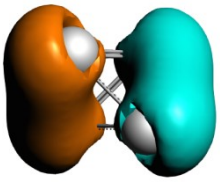 t_2, E = -0.4406	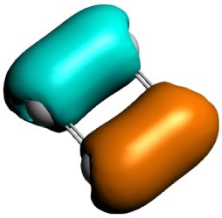 e_{1u}, E = -0.4611	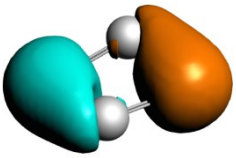 b, E = -0.4717	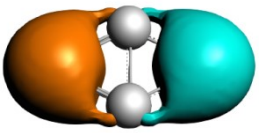 b_u, E = -0.4760
HOMO	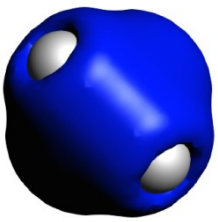 a_1, E = -0.5699	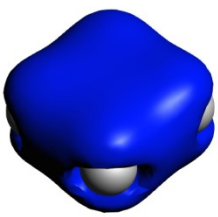 a_{1g}, E = -0.5468	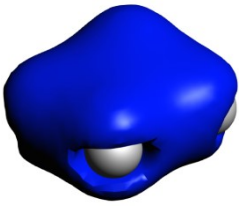 a, E = -0.5450	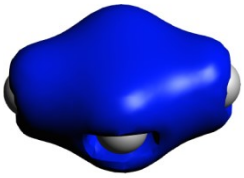 a_g, E = -0.5459

Table S8. The calculated NICS values (ppm) of the Ag_4^{2+} cluster

Structure	Number of Bq_x[a]	NICS (ppm)[b]
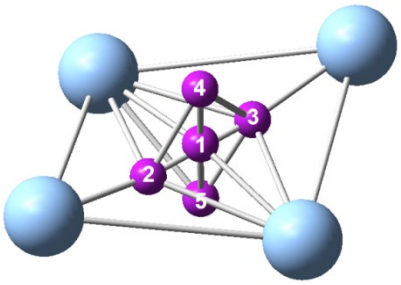	1	-15.9
	2	-16.4
	3	-16.4
	4	-8.3
	5	-9.7

[a] Bq_x represents the ghost atom with numbering x. [b] For benzene: -8.0 ppm at the center and -10.2 ppm at 1 Å above the ring plane)

Table S9. Constrained DFT optimization results of the $[Ag_4]^{q+}$ core in the experimental cavity of 7DC1.

Specie	Total Charge	q	Geometry Structure							
			Bond Length (Å)						Dihedral Angle (°)	
			Ag1-Ag2	Ag1-Ag4	Ag2-Ag3	Ag3-Ag4	Ag1-Ag3	Ag2-Ag4	Ag1-Ag2-Ag4-Ag3	Ag2-Ag1-Ag3-Ag4
Ag_4-$(Atox1)_2$ 7DC1 (Experiment)			2.83	3.17	3.17	2.83	3.65	4.68	150.8	157.0
$[Ag_4]$ in cavity of 7DC1	0	+4	3.02	3.26	3.22	2.96	4.19	4.59	166.3	167.4
	-2	+2	3.03	2.96	2.91	3.02	4.10	4.21	151.8	152.5
	-4	0	null (not converged)							

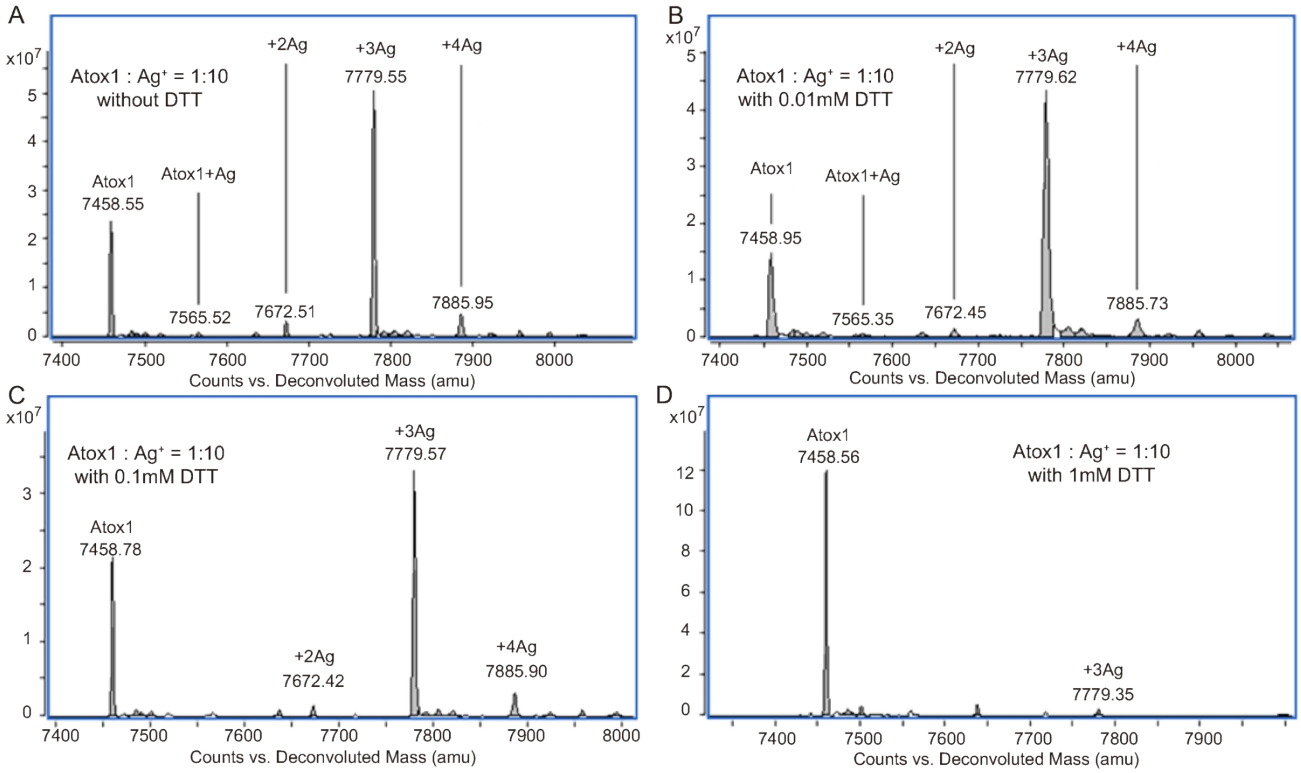

Figure S1. The liquid chromatography electrospray ionization tandem mass spectrometry (LC-ESI-MS) measurement of Atox1 and silver ions. (A) LC-ESI-MS of Atox1 protein (Found: 7458.55Da, expected: 7458.94Da) and Atox1 in complex with different equivalents of Ag ion. (B) (C) (D) ESI-MS of Atox1 protein and Atox1 in complex with different equivalents of Ag ion in the different buffer conditions including 0.01 to 1 mM DTT.

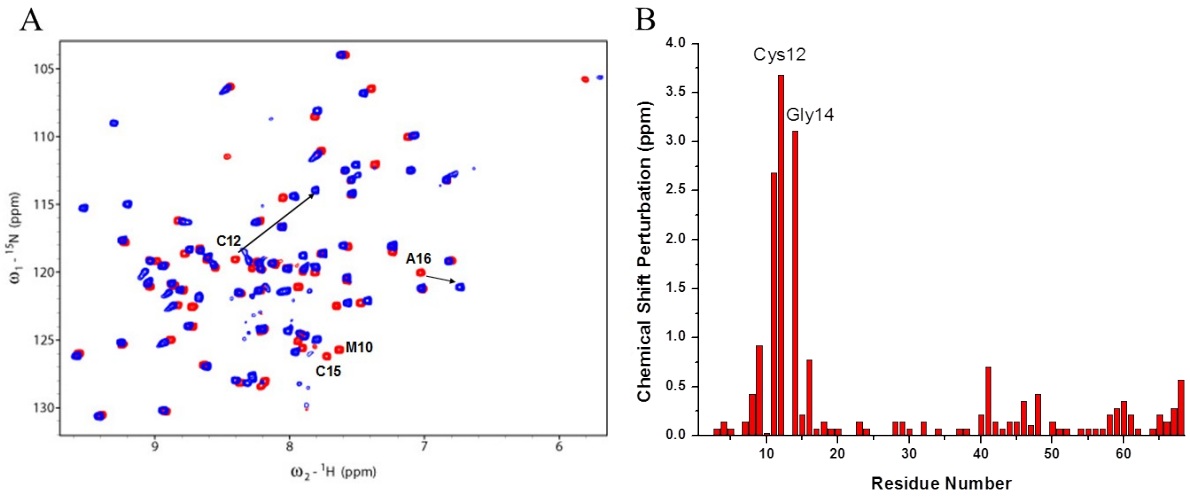

Figure S2. NMR analysis of Ag^+ binding to Atox1. (A) Overlay of $^1H,^{15}N$-HSQC NMR spectra of Atox1 apo-Atox1 before (red) and after (blue) adding equimolar Ag^+. (B) Chemical shift perturbation Δδ against the residue number ($\Delta\delta = \sqrt{[(\Delta\delta_H)^2 + (\Delta\delta_N / 5)^2]/2}$).

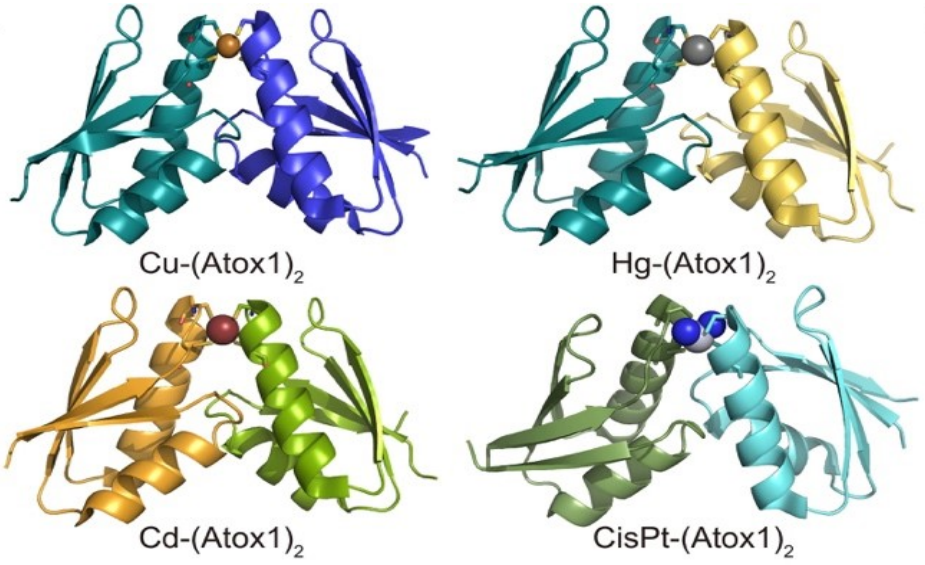

Figure S3. Atox1 crystal structures in the presence of metals (Cu-Atox12 PDB accession code 1FEE, Hg-Atox12 PDB accession code 1FE4, Cd-Atox12 PDB accession code 1FE0, CisPt-Atox12 PDB accession code 3IWX).

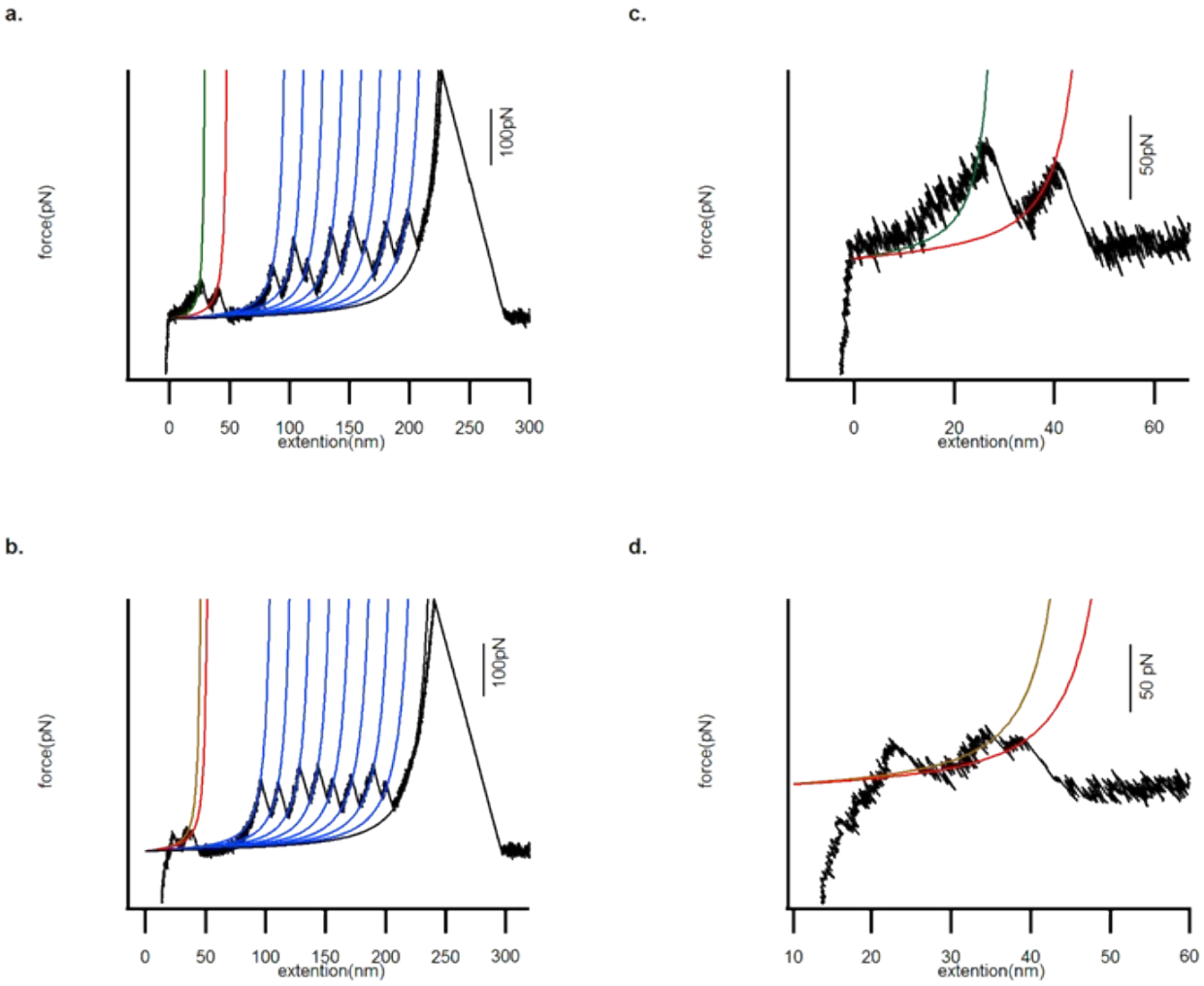

Figure S4. The rare cases we observed in the single-molecule force spectroscopy experiments. The SMFS measurements on the engineered chimeric polyprotein in the presence of Ag, and the rupture of Ag4-(Atox1)2 complex proceeded in two steps.

Figure S5. Reported Atox1 crystal structures in the presence of metals and Ag_4-$(Atox1)_2$ in this work. Crystal structure of Ag bound to an Atox1 dimer with 2.70 Å (PDB accession code 5F0W).

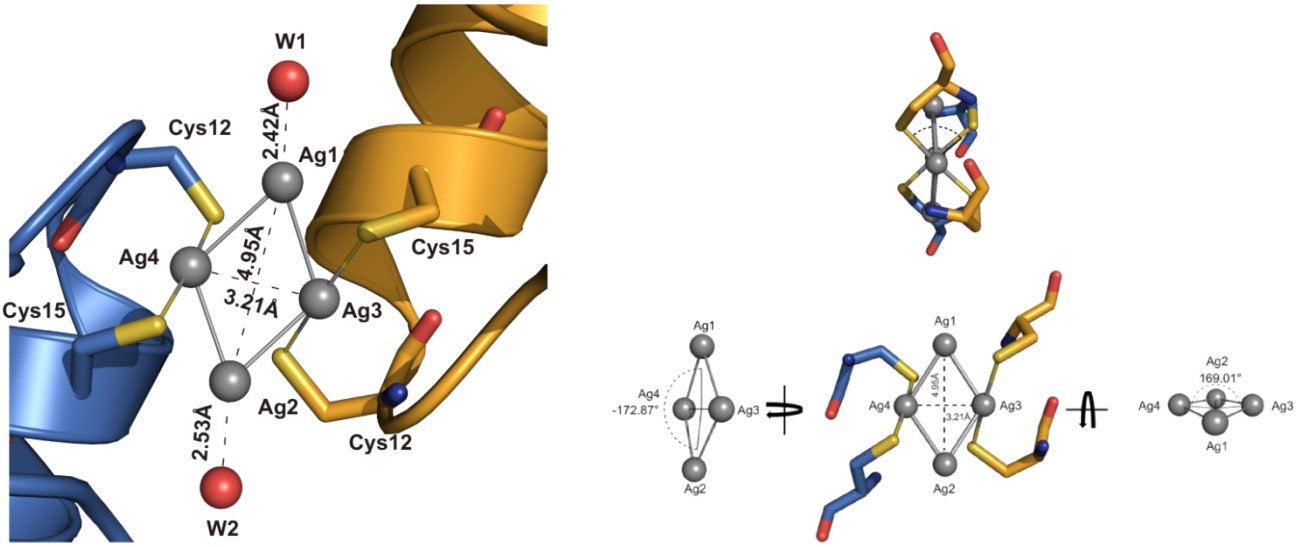

Figure S6. Close-up view showing details of the tretrasilver cluster in Atox1 dimer(5F0W). The distance between Ag1 and Ag4 is 3.01 Å. The distance between Ag1 and Ag3 is 2.95 Å. The distance between Ag2 and Ag3 is 2.95 Å. The distance between Ag2 and Ag4 is 2.89 Å. The Angle Ag4-Ag1-Ag3 is 65.01°, and the angle Ag4-Ag2-Ag3 is 66.56°. The four silver ions are situated nearly on the same plane, forming four Ag-Ag bonds with an average dihedral angle of 171º.

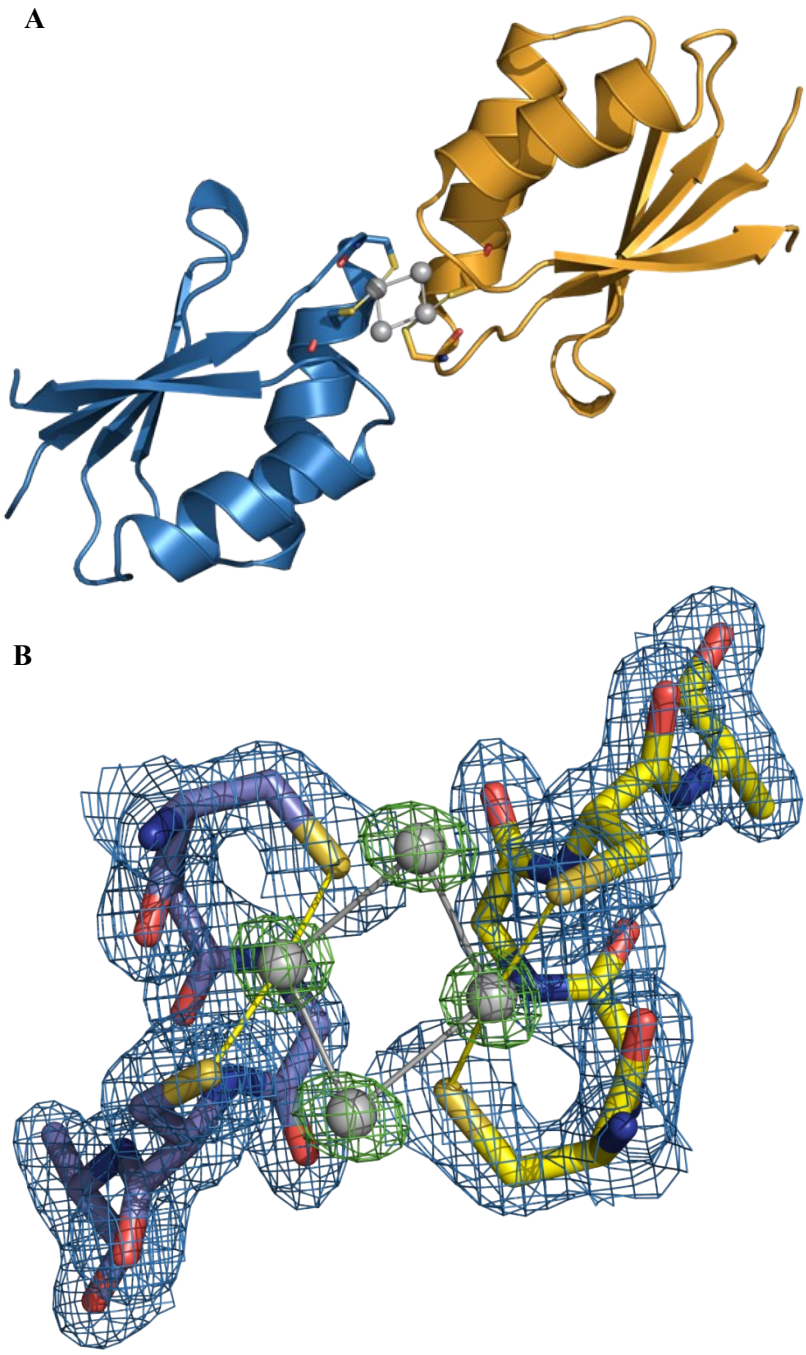

Figure S7. (A) Crystal structure of Ag bound to an Atox1 dimer with 1.75 Å (PDB accession code 7DC1). (B) The superimposed 2*Fo-Fc* electron density map of Ag_4-$(Atox1)_2$. 2*Fo-Fc* electron density map (gray, 1.00σ) of Ag4-(Atox1)2 metal center with anomalous difference Fourier density showing the Ag ions superimposed (green, 6σ).

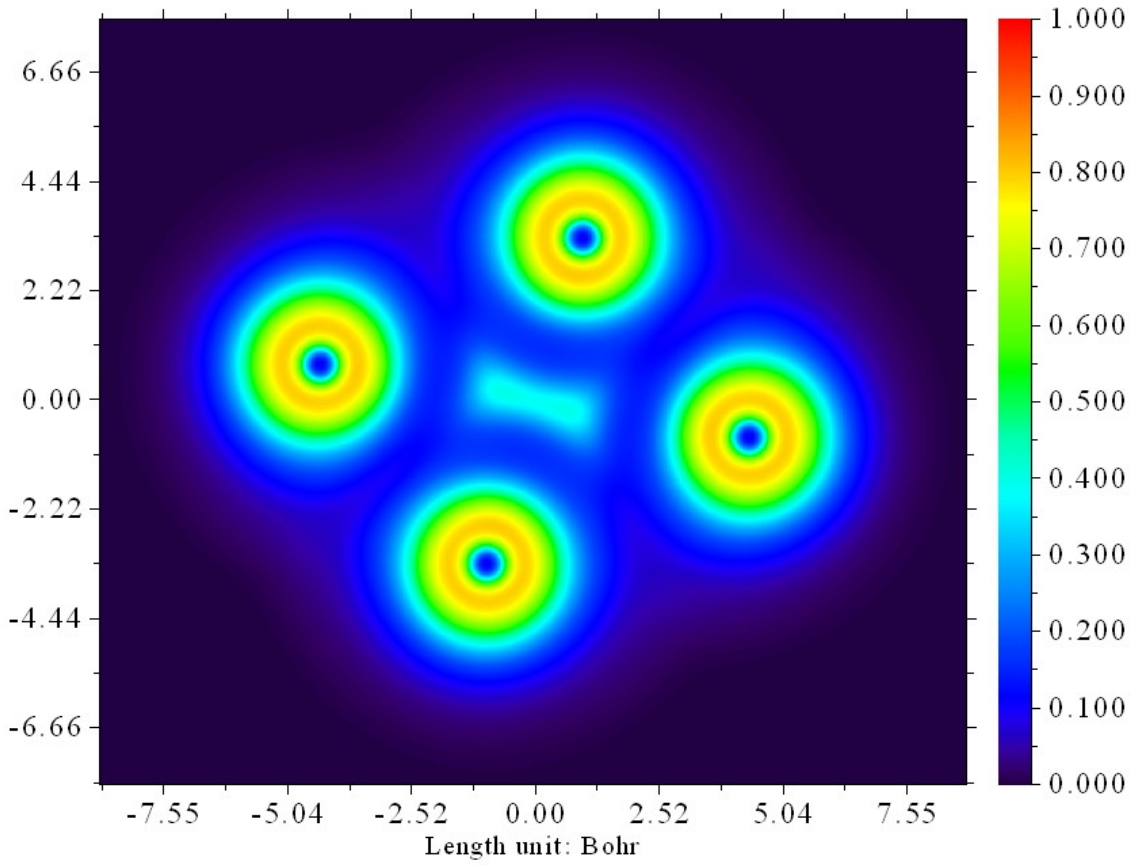

Figure S8. The ELF color-filled map of Ag_4^{2+} generated by Multiwfn. Significant electron-pair density in the center of the cluster supported delocalized 4-center weak bonding.

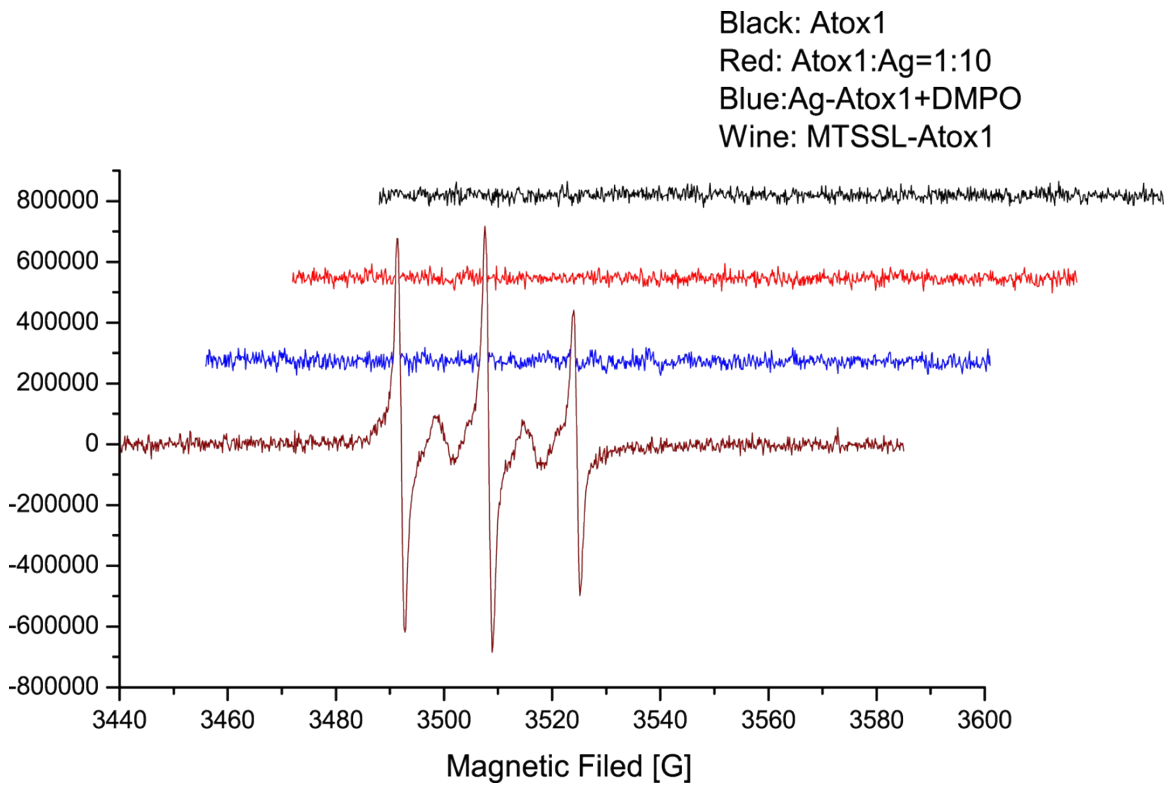

Figure S9. The CW-EPR spectra mesurement of Atox1, Atox1-Ag, Ag-Atox1 with DMPO and MTSSL-Atox1.

References

1. W. Wei, Y. Sun, M. Zhu, X. Liu, P. Sun, F. Wang, Q. Gui, W. Meng, Y. Cao and J. Zhao, *J Am Chem Soc*, 2015, **137**, 15358-15361.
2. S. R. Ainavarapu, J. Brujic, H. H. Huang, A. P. Wiita, H. Lu, L. Li, K. A. Walther, M. Carrion-Vazquez, H. Li and J. M. Fernandez, *Biophys J*, 2007, **92**, 225-233.
3. I. C. Shaw, *Chem Rev*, 1999, **99**, 2589-2600.
4. S. Chernousova and M. Epple, *Angew Chem Int Edit*, 2013, **52**, 1636-1653.
5. G. B. Song, F. Tian, H. X. Liu, G. Q. Li and P. Zheng, *J Phys Chem Lett*, 2021, **12**, 3860-3867.
6. G. D. Yuan, H. X. Liu, Q. Ma, X. Li, J. Y. Nie, J. L. Zuo and P. Zheng, *J Phys Chem Lett*, 2019, **10**, 5428-5433.